sustainability

MDPI

Article

Thermal Performance of Novel Eco-Friendly Prefabricated Walls for Thermal Comfort in Temperate Climates

Rafael Alavez-Ramirez [1], Fernando Chiñas-Castillo [2,*], Jacobo Martínez-Reyes [3], Jose Luis Caballero-Montes [1], Magdaleno Caballero-Caballero [1], Valentin Juventino Morales-Dominguez [1], Margarito Ortiz-Guzman [1], Luis Humberto Robledo-Taboada [2], Erick Adrian Juarez-Arellano [4] and Laura Elvira Serrano-De la Rosa [5]

1 Instituto Politecnico Nacional, CIIDIR Unidad Oaxaca, Hornos No. 1003, Col. Noche Buena, Santa Cruz Xoxocotlan C.P. 71230, Mexico; ralavez@ipn.mx (R.A.-R.); jcaballerom@ipn.mx (J.L.C.-M.); mcaballero@ipn.mx (M.C.-C.); valentin_md@yahoo.com.mx (V.J.M.-D.); mortizgu@ipn.mx (M.O.-G.)
2 Instituto Tecnologico de Oaxaca, Tecnologico Nacional de Mexico, Calz. Tecnologico No. 125, Oaxaca C.P. 68030, Mexico; luis.rt@itoaxaca.edu.mx
3 Instituto Politecnico Nacional, Escuela Superior de Ingenieria Mecanica y Electrica, Unidad Profesional Adolfo Lopez Mateos, Col. Linda Vista, Del. Gustavo A. Madero C.P. 07300, Mexico; jacobomartinezreyes@gmail.com
4 Centro de Investigaciones Científicas, Instituto de Química Aplicada, Universidad del Papaloapan, Circuito Central 200, Parque Industrial, Tuxtepec C.P. 68301, Mexico; eajuarez@unpa.edu.mx
5 Instituto de Fisica, Benemerita Universidad Autonoma de Puebla, 14 sur y Av., San Claudio C.P. 72570, Mexico; lauras@ifuap.buap.mx
* Correspondence: fernandochinas@itoaxaca.edu.mx; Tel.: +52-19511838112

Abstract: The global threat of climate change has become increasingly severe, with the efficiency of buildings and the environment being significantly impacted. It is necessary to develop bioclimatic architectural systems that can effectively reduce energy consumption while bringing thermal comfort, reducing the impact of external temperatures. This study presents the results of a real-scale experimental house prototype, MHTITCA, using a unique design composed of novel eco-friendly prefabricated channel walls filled with a blend of soil, sawdust, and cement for walls and roofs. The experimental analysis performed in this study was based on dynamic climatology. A solar orientation chart of the place was constructed to identify the solar radiation intensity acting on the house. Measurements of roof surface temperatures were conducted to determine temperature damping and temperature wave lag. Monthly average temperature and direct solar radiation data of the site were considered. Compared to other alternative house prototypes, the system maximizes thermal comfort in high-oscillation temperate climates. Temperature measurements were taken inside and outside to evaluate the thermal performance. A thermal insulating layer was added outside the wall and the envelope to improve the prototype's thermal comfort and reduce the decrement factor even more. This MHTITCA house prototype had 85% thermal comfort, 0% overheating, and 15% low heating. This eco-friendly prototype design had the best thermal performance, achieving a thermal lag of twelve hours, a reduced decrement factor of 0.109, and preventing overheating in areas with high thermal fluctuations. Comparatively, the other prototypes examined provided inferior thermal comfort. The suggested MHTITCA system can be an energy-saving and passive cooling option for thermal comfort in low-cost houses in temperate climates with high thermal oscillations in urban or rural settings.

Keywords: thermal inertia; passive cooling; sustainability; climatic change; thermal performance

Citation: Alavez-Ramirez, R.; Chiñas-Castillo, F.; Martínez-Reyes, J.; Caballero-Montes, J.L.; Caballero-Caballero, M.; Morales-Dominguez, V.J.; Ortiz-Guzman, M.; Robledo-Taboada, L.H.; Juarez-Arellano, E.A.; Serrano-De la Rosa, L.E. Thermal Performance of Novel Eco-Friendly Prefabricated Walls for Thermal Comfort in Temperate Climates. *Sustainability* **2024**, *16*, 9349. https://doi.org/10.3390/su16219349

Academic Editor: Giouli Mihalakakou

Received: 13 September 2024
Revised: 15 October 2024
Accepted: 24 October 2024
Published: 28 October 2024

1. Introduction

The global threat of climate change has become increasingly severe, with the efficiency of buildings and the environment being significantly impacted [1]. This has led many

countries to adopt energy efficiency policies [2]. The residential sector, in particular, is a significant energy consumer worldwide. It is, therefore, imperative to develop and implement bioclimatic architectural systems that can effectively reduce energy consumption without compromising the thermal comfort of the building [3]. According to Wegertseder et al. [4], the residential sector alone is responsible for a staggering 40% of the emissions generated on the planet. In a typical home, air conditioning alone can account for between 40% and 60% of the average energy consumption, underscoring the need for energy-saving measures in the residential sector.

Understanding the thermal properties of construction materials used in buildings is crucial in reducing the impact of external temperatures. Architects need to comprehend climate behavior to create the ideal construction system. Sadly, this is not a common practice in current Latin American architecture. Architects often ignore weather conditions and utilize improper practices, particularly in rural homes. For instance, they still use imported or endemic materials in temperate climates, even if these materials do not possess the necessary properties to ensure thermal habitability. Builders, engineers, architects, and official bodies frequently use unsuitable materials for their context, compromising the residents' comfort. Thermal comfort is crucial as it is the "condition of mind that expresses satisfaction with the thermal environment" [5]. ANSI/ASHRAE 55 [6] states, "It is determined from subjective evaluations". It is one of the critical aspects of user satisfaction and energy consumption in buildings, considering that modern man spends most of his time indoors. The thermophysical properties of construction materials are vital in minimizing thermal gains by radiation or conduction or storing thermal energy for comfort conditions and energy savings. Six fundamental factors define internal comfort conditions: metabolic rate, clothing insulation (clo), air temperature, radiant temperature, air velocity, and humidity [6].

When constructing low-cost houses, the primary focus is often on selecting materials with the lowest price without considering their thermal performance according to the local climate conditions. However, it is essential to consider bioclimatic design strategies, such as using materials with high thermal inertia, to regulate indoor temperatures and reduce fluctuations in places such as Oaxaca City, which has a temperate climate plus high thermal oscillation. In Latin America, adobe is a traditional material used to construct house walls, especially in rural areas. This material is eco-friendly due to the handling and manufacturing process. However, its structural value is often undermined due to its poor performance in earthquakes and floods, and construction regulations do not recognize it. As a result, adobe technology has been replaced with modern materials such as concrete, brick-fired, or steel.

The term thermal inertia is used in [7] to describe the general ability of a building to store and release heat. The greater the thermal inertia of a building, the slower the rate at which the internal temperature rises and falls. Therefore, the thermal inertia of a building system should be considered to reduce the heat flow and induce thermal damping in small buildings exposed to thermal oscillations higher than 10 °C. Thermal inertia or thermal mass is usually associated with the construction mass of the building itself. It is generally contained in the walls, partitions, ceilings, and building floors, built with high-heat capacity materials. Thermal inertia is a thermophysical property that represents a material's ability to conduct and store heat. It is related to thermal conductivity and volumetric heat capacity. In contrast, heat transfer in buildings is related to how fast or slow heat transfer takes place.

The location and distribution of thermal mass are also important, so adding thermal mass to the building is insufficient. Huelsz et al. [8] showed that selecting an insulating material for the envelope element of high thermal resistance can have detrimental effects on the thermal performance of the building; this is because an insulating material cannot store and release thermal energy. Thus, to achieve an excellent indoor microclimate in homes, thermal mass is as critical as thermal insulation [8].

Youcef Ettoumi et al. [9] consider that buildings must have high thermal inertia to achieve a comfortable room temperature. However, thermal inertia depends not only on

the time interval and the decay factor but also on a complex interaction between material density, specific heat capacity, and thermal conductivity. Temperature variations will be reduced in a thermally heavy building, where high inertia improves continuously heated buildings' comfort and thermal behavior [10]. The thermal inertia of a building depends directly on the thermal capacity, counteracting all sudden temperature changes and reducing and postponing the effects of the external condition (thermal lag and decrement factor).

Various research studies have evaluated the effectiveness of thermal inertia in different climates concerning thermal comfort and energy consumption [11–17]. It has been suggested that the thermal inertia of a building should be a prerequisite for architectural design in hot climates [18]. Other studies have stated that thermal inertia can also be helpful in cold climates [16]. Shavid et al. [17] calculated the influence of thermal mass and night-time ventilation on maximum indoor temperatures, assuming that indoor temperature is linearly related to outdoor thermal oscillation and night-time ventilation rates. The study simulated four scenarios in test chambers: (1) without night ventilation, (2) with natural night ventilation, (3) with forced ventilation, and (4) with four levels of thermal mass and ventilation rates. The results showed that a reduction between 3 and 6 °C is possible in a high-thermal-mass building without operating an air conditioning unit in a hot and humid climate.

Ogoli [19] analyzed buildings with low and high thermal mass that effectively lowered maximum interior temperatures below exterior temperatures. Studies conducted by Medjelekh et al. [15] have revealed the effectiveness of thermal inertia in hot and sub-humid climates to create hygrothermal comfort and reduce building energy consumption. Under contrasting environments characterized by cold winters and hot summers, the positive contribution of thermal inertia has ranged from approximately 6% for heating to 21% for cooling [20].

Flores et al. [13] analyzed the thermal and energetic behavior of two single-family houses, a massive house, and a lighthouse in the central region of Argentina during summer. Both constructions were monitored simultaneously between December 2006 and January 2007. The results show that for an average outside temperature of 26.3 °C during the entire period, the average temperature in the house was 27.6 °C without air conditioning. At the same time, the inside of the lighthouse had an average temperature of 26.8 °C but included a period with air conditioning. It is essential to accentuate natural, cross, and selective ventilation in the summer to minimize conventional energy consumption and dimensionalize the storage mass correctly for light constructions.

Filippin et al. [21] analyzed the thermal behavior of houses built by the IPV (Provincial Housing Institute) in Salta, Argentina, for a typical day in winter and summer. In winter, the average interior temperatures of the houses oscillate around 14 °C, with thermal amplitudes between 5 °C and 10 °C. This is clearly outside the comfort zone, for which conventional auxiliary heating is necessary throughout the day. In summer, the dwellings are outside of the thermal comfort zone for most of the day, with interior temperatures higher than exterior temperatures and daily thermal amplitudes oscillating between 7 and 10 °C.

Filippin et al. [12] evaluated the summer thermal behavior of four massive and compact dwellings in low-density urban areas in Santa Rosa, Argentina. The monitoring comprised twelve days in February 2010 with an average indoor temperature of 23.3 °C, maximum outdoor temperatures above 30 °C, and solar irradiance close to 900 W/m^2. The average interior temperature of the houses without mechanical conditioning was 27.1 °C, and 5.2 kW/h of electrical energy was consumed daily. Gallegos-Ortega et al. [14] analyzed the delay time and thermal damping of a house with straw bales in Baja California, Mexico. The results showed that the thermal lag was 9.12 h and an interior temperature of 25.6 °C. Alavez-Ramirez et al., in previous work, evaluated bricks with soil–cement–sawdust, finding a thermal damping value of 81.5%, a decrement factor of 0.166, and a thermal lag of 7:30 h compared with concrete components [11].

In this work, the authors evaluated the thermal performance through measurements of thermal time lag and decrement factor in a modular full-scale eco-friendly prototype

house (MHTITCA) of a novel prefabricated channel based on reinforced mortar filled with soil–sawdust fiber–cement combined with insulation to maximize thermal comfort and stability. The authors of this paper decided to carry out thermal monitoring in situ on a full-scale dwelling to measure temperature values coming from the heat transmission mechanisms present (radiation, conduction, and convection). Thus, the technique applied in the present paper is believed to be more realistic. The house prototype design is focused on low-cost housing use, and its performance was compared with three other typical alternative house prototypes.

2. Materials and Methods

2.1. Climatic Characterization

The research work described in this paper was carried out in Oaxaca. Oaxaca is located in the southeast part of the Mexican Republic at geographic coordinates of 17°04′59″ N latitude and 96°42′35″ W longitude. It has an altitude of 1550 m above sea level with a mild climate, a mean temperature of 22 °C, and an annual thermal oscillation of 16.8 °C [22]. At the start of this research work, a climatic and bioclimatic analysis of weather data from Oaxaca City was carried out to determine the variables that influence the dynamic thermal behavior of the tested prototypes using meteorological data.

Figure 1 shows that the city of Oaxaca has a temperate bioclimate (white) and falls in the thermal comfort range of 21 to 26 °C with a total annual rainfall of 783.5 mm. The National Water Commission collected primary data from weather stations in Mexico and provided the data for the climate classification [23].

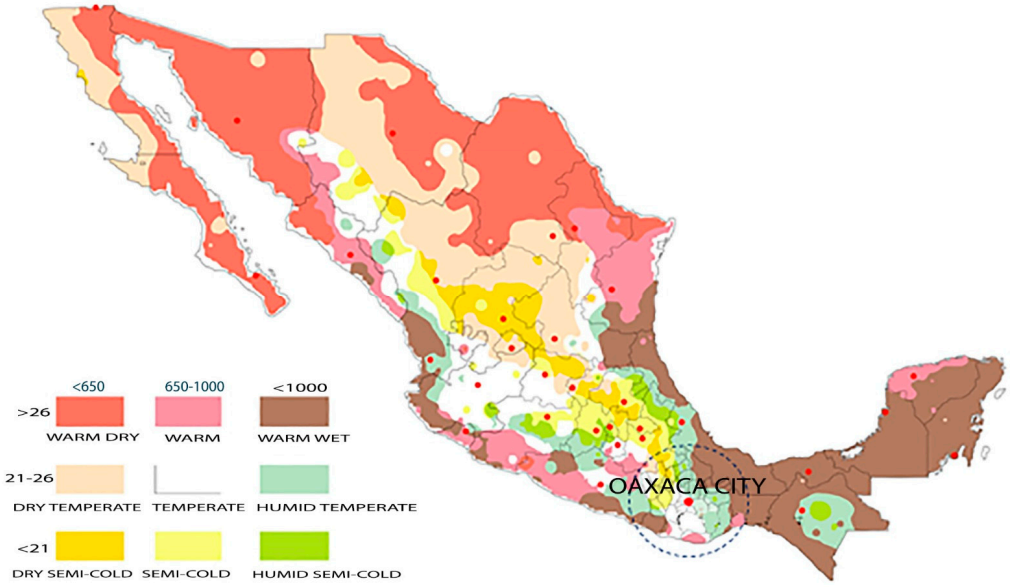

Figure 1. Bioclimatic classification of the Mexican Republic [22].

2.2. Prefabricated Eco-Friendly Channels and Experimental Prototypes

The real-scale experimental eco-friendly house prototype (MHTIT) and the other full-scale house prototypes used for comparison purposes were built and located at the IPN CIIDIR Oaxaca Unit facilities. This house prototype, MHTIT, consisted initially of a prefabricated wall and roof system. A metal formwork system was built, allowing wall and roof components to be prefabricated. Figure 2a shows the construction of prefabricated channels for walls with dimensions of 1.35 × 0.6 × 0.025 m LWH. Figure 2b shows the structure of the prefabricated channels for the roof system with dimensions of 2.70 × 0.6 × 0.025 m LWH.

(**a**) (**b**)

Figure 2. Preparation of prefabricated channels: (**a**) for the walls and (**b**) for the roof.

The soil was conditioned before constructing channels and preparing the fillers for the channels proposed in this study. A mixture of sandy clay soil and 10% cement was used to stabilize the soil, and tracks were filled with reinforced mortar for walls. This ratio was recommended by several authors, including Bahar et al. [24] and Roseto [25]. Four mixtures were prepared to fill the channels, adding cement, sawdust wood, and soil. It aimed to achieve a low specific weight for the channel filling that would suit the slabs. The 774.1 kg/cm^2 soil exhibited the lowest wet volumetric weight. An axial compression test was conducted using the NMX-C-037-ONNCCE, 2005 [26] to evaluate the strength and durability of the mixtures for the roof channels. The test was performed at 32 °C, with a relative humidity of 28 ± 2%, and consisted of five replicate samples. The axial compression tests used the Geotest Instrument Corp S5830 Multiloader with an end scale of 50 kN. The filler material had a strength of 0.759 kg/cm^2.

Figure 3a shows the MHTIT experimental prototype. The thermal inertia-focused building's wall and roof, measuring 3.84 m in length and 2.76 m in width, is oriented north to south, with all four facades receiving direct sunlight and with the access door on the north side. The floor has a 10-centimeter thickness and is made from a cement–soil mix in a 1:10 ratio. Walls and roofs are prefabricated, using cement–sand mortar reinforced with electro-welded mesh and chicken wire. Wall channels were cast with soil, sawdust fiber, and 10% cement, with the thickness totaling 0.2 m. The ceiling utilizes the same filler mixture, while the roof uses a 0.025 m thick reinforced cement–sand mortar slab and a red clay half-slab brick layer finished with cement plaster. Figure 3b illustrates the isometric view of the MHTIT system's material and measurement layers in the wall and roof design.

Figure 4 shows an isometric view of the MMTLM of the house with a construction system of reinforced mortar walls and empty milk boxes, known as Tetra Pak, and a reinforced mortar slab. The house has a surface area of 28.55 m^2, the orientation of the house is north–south, the access door faces south, and it has two windows, one exposed to the south and another to the north. The blind walls are presented in the east–west direction like the other houses; the floor is made of concrete 0.1 m thick. The slab and wall system comprises reinforced mortar channels with variable lengths (2.8 to 3.50 m), widths of 0.5 m, and thicknesses of 0.03 m. Empty milk boxes (Tetra Pak) were placed inside the channels used on the walls.

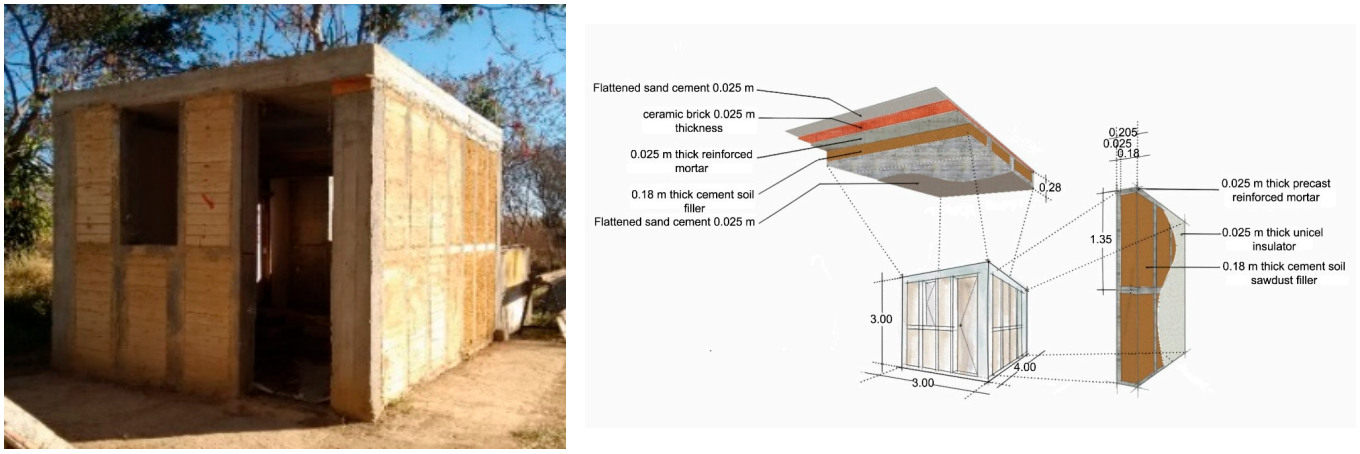

(**a**) (**b**)

Figure 3. MHTIT experimental module: (**a**) MHTIT prototype and (**b**) isometric view of the MHTIT.

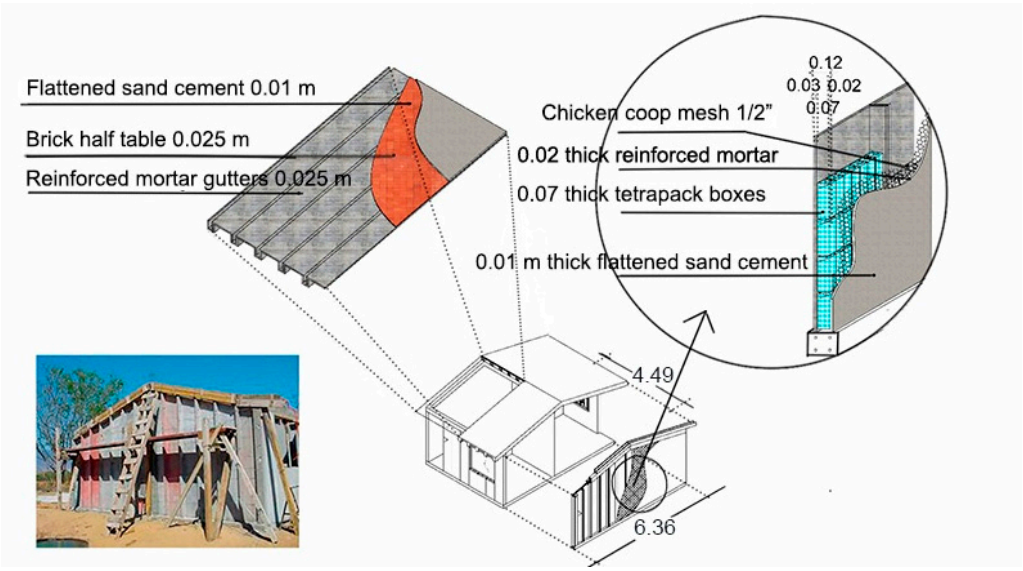

Figure 4. Isometric view of the MMTLM house with reinforced mortar walls, empty milk cartons (Tetra Pak), and a reinforced mortar slab.

The isometric view of the MBSCLM house is shown in Figure 5. The house has a brick wall, compacted soil, and a reinforced mortar slab. Its total surface area is 28.92 m^2 and faces the north–south direction. The entrance to the house is located on the southern side, and there are two windows—one facing south and the other facing north. The east–west walls are blind, similar to the other houses. The house floor is made of 0.1 m thick concrete, and the slab system comprises reinforced mortar channels with variable length sections ranging from 3.0 to 3.50 m, a width of 0.5 m, and a thickness of 0.03 m. The wall system includes soil blocks compacted with 8% cement and has a block section of 7 × 14 × 28 cm.

The MMLM house is shown in Figure 6 from an isometric view, featuring a reinforced mortar construction system. The house spans an area of 53 m^2 with a north–south orientation and south-facing door access. It has three windows, one facing east and two facing north. The floor has a thickness of 0.10 m, and the slab and wall system is constructed using sand cement mortar reinforced with 10/10 gauge and 3/8 rods, with a grid distribution of 1 m spacing.

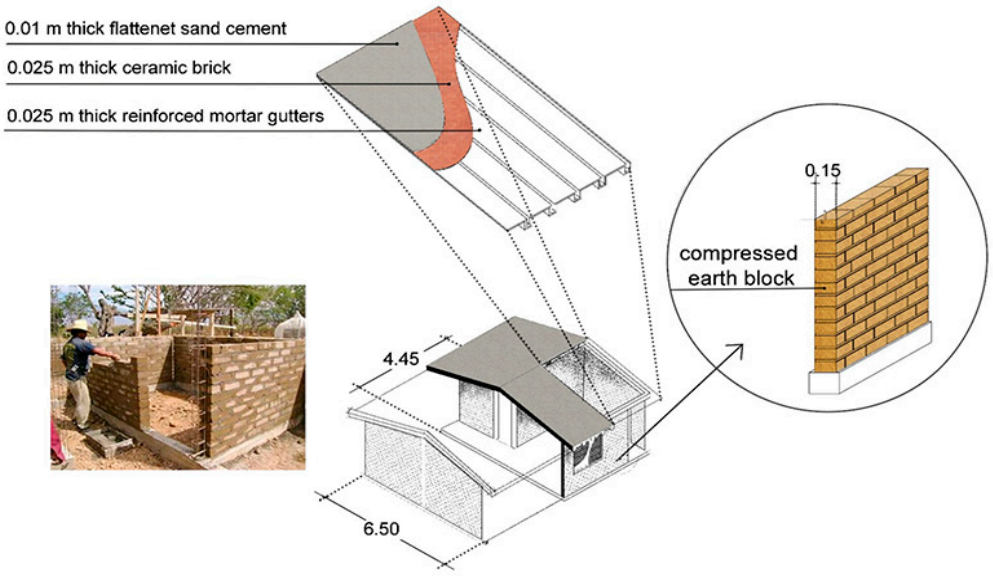

Figure 5. Isometric view of the MBSCLM house with compacted soil block walls and a reinforced mortar slab.

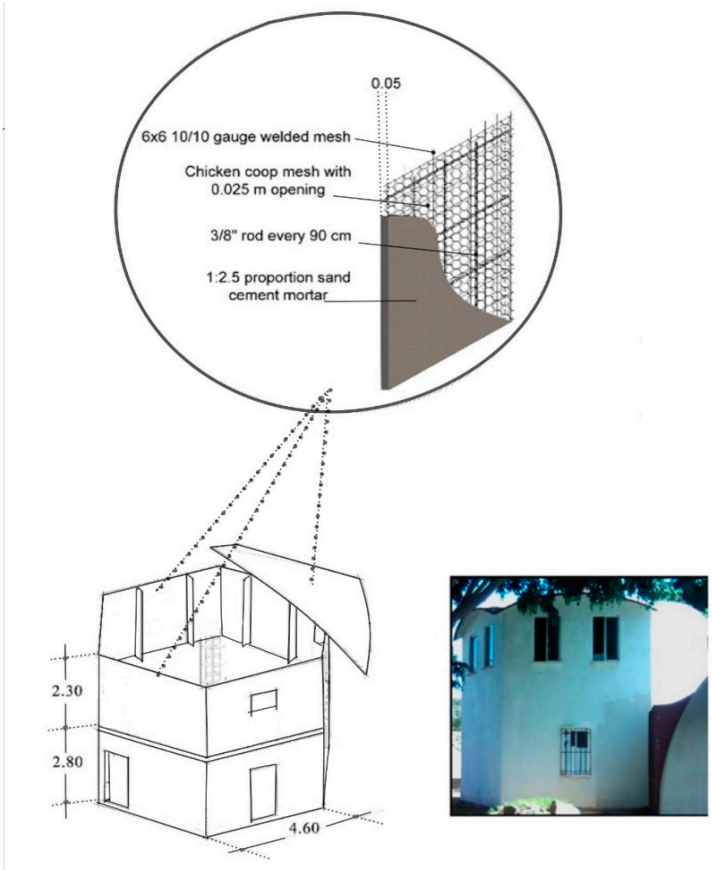

Figure 6. Isometric view of the MMLM house with reinforced mortar.

2.3. Evaluation of the Thermal Performance of Experimental Prototypes

Thermal monitoring was carried out inside the housing prototypes, and air temperature measurements were taken at hourly intervals inside and outside the house. The temperatures recorded inside the prototypes built were compared to the local thermal comfort temperatures and the outside ambient temperature. Figure 7 indicates that the highest temperature throughout the year 2023 occurred in April.

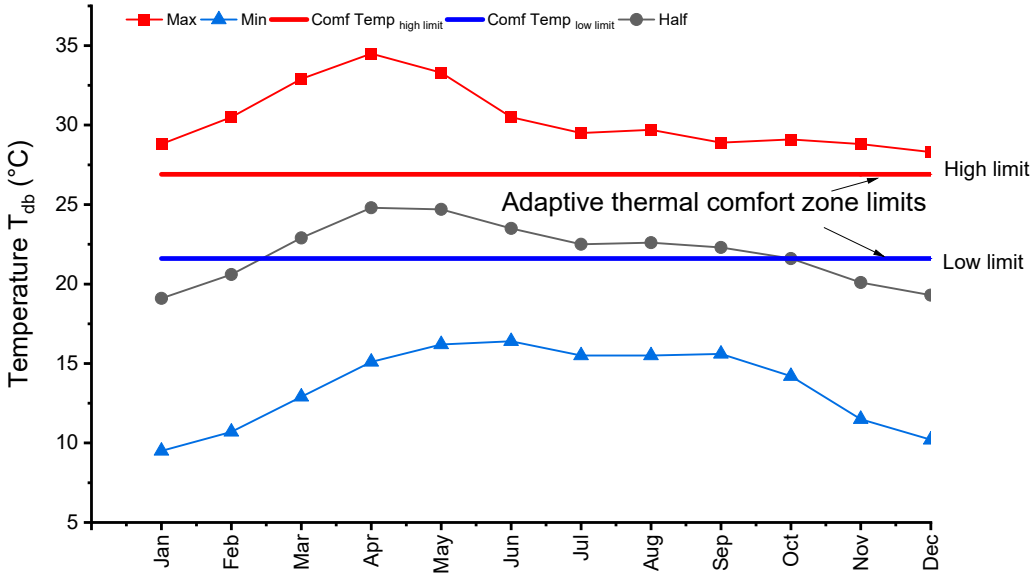

Figure 7. Monthly temperatures in the city of Oaxaca.

The temperature measurements were recorded at the geometric center of each prototype house at the occupants' height. Thermal monitoring was started simultaneously in the four places, and a thermal coat was used to take measurements outside. The monitored houses did not have any conventional cooling systems. The hobos used to carry out the measurements were type U12-006, which includes the HOBOware Pro software and a Calibration Kit and stores 43,000 measurements with a sampling range of 1 s–18 h.

The percentages of thermal comfort, low heating, and overheating were determined by considering the interior temperatures recorded in the house prototypes under study.

The prototypes' decrement factor was also determined during April's four hot and stable days.

The decrement factor (thermal damping) is the relationship between the maximum temperature difference inside the construction system and the maximum difference of the ambient outside temperature (thermal amplitude). The effectiveness of the thermal performance of the house prototypes under study was determined through its decrement factor using the following equation.

$$\mu = \Delta T_{In} / \Delta T_{Out} \quad (1)$$

where μ is the decrement factor of the house prototype, ΔT_{In} is the difference between the maximum and minimum temperatures reached inside, and ΔT_{Out} is the difference between the maximum and minimum temperatures reached outside.

Thermal time lag (also called time delay) was determined using the difference between the time of maximum inner surface temperature recorded inside the house prototype and the time of maximum outer surface temperature of the wall. Materials with long thermal lag times will absorb and release heat slowly, while materials with short thermal lag times will absorb and release heat quickly. The thermal time lag was determined using the following equation.

$$TL = t_{T_{in,max}} - t_{T_{out,\ max}} \quad (2)$$

where $t_{T_{in,max}}$ is the time of maximum inner surface temperature and $t_{T_{out,max}}$ is the time of maximum outer surface temperature.

2.4. Evaluation of the Equivalent Thermal Conductivity

Thermal conductivity measurements were conducted using a fully equipped hot plate thermal conductivity testing system for the real-scale constructive component MHTITCA

of 1 m^2, and the main thermal properties were calculated. While the complete dataset is not included in this paper, it can be made available upon request.

The apparatus consists of a box with one side open, in which heat is generated using an electric heating system. The walls of the box are thermally insulated with a ceramic fiber material. This is a primary apparatus that uses steady-state conduction heat transfer as a principle and allows for the determination of thermal conductivity according to ASTM C 177.

To determine thermal conductivity, the constructive components are mounted on the open side and the box is completely closed. A constant heat flow of 100 W is supplied to the specimen with an area of 1 m^2 through a controlled power supply and wire resistance attached to a 6 mm AISI 1018 hot plate.

3. Results

3.1. Climate Characterization

Throughout April 2023, indoor temperatures were recorded on-site every hour for the house prototype module (MHTIT) and compared against the other alternative systems with the same climatic conditions. The local polygon of thermal comfort, which ranges between 21 °C and 26 °C, was used as a benchmark for comparison. Each system's overheating, thermal comfort, and underheating percentage were calculated based on the recorded temperatures. Overheating was defined as temperatures exceeding the thermal comfort range (26.92 °C), while underheating was defined as temperatures below the thermal comfort zone.

The temperature data used to determine the thermal comfort zone of Oaxaca City were obtained from the climatological normals of station 00020079 Oaxaca. The station's geographic coordinates (latitude: 17°04′59″ N, longitude: 096°42′35″ W, height: 1594 MASL) were used to collect data from Servicio Meteorologico Nacional (Mexico's national weather organization) [23]. Temperatures taken into account were representative of winter and summer seasons. From these data, maximum, minimum, and average monthly values were obtained. Mean temperature data were used to determine the neutral temperature and comfort zone of the locality using a model from the Auliciems and Szokolay equation model based on Equations (3) and (4) [27].

$$Tn = 17.6 + 0.31\ Tm \quad (3)$$

$$Tcz = Tn \pm 2.5 \quad (4)$$

where Tn = neutral temperature (°C), Tm = average temperature (°C), and Tcz = temperature of the thermal comfort zone (°C). Therefore, the calculated mean temperature for Oaxaca was 22 °C, and the estimated annual neutral temperature was 24.42 °C. The thermal comfort zone at the site was determined to be between 21.92 °C and 26.92 °C. This methodology uses the adaptive model of thermal comfort. Figure 7 shows the temperatures and limits of the thermal comfort zone. This thermal comfort range is considered for people acclimatized to the site (Adaptive Thermal Comfort Model). Among the current thermal standards applicable to the built environment, the adaptive model provides greater flexibility to adapt indoor comfort temperatures to the outdoor climate, particularly in naturally ventilated buildings. Adaptive standards are considered more appropriate for establishing comfort in low-energy buildings.

According to Figure 8, the rainy season in Oaxaca lasts from May to September, with the highest rainfall in June. Figure 9 details the hourly temperatures in the area, shown on a chromatic scale representing the thermal comfort zone (ranging from 21.9 to 26.9 °C). Overheating is indicated at 29.5%, underheating at 50%, and the thermal comfort zone at 20.5%. Figure 10 shows that humidity levels in the study area are relatively stable throughout the day, with an increase during the night (between 1:00 and 8:00 p.m.) from May to October, extending until 9:00 a.m. This increase in humidity is due to an increase in cloudiness and moisture in the environment, which also leads to a decrease in solar

radiation and rainfall in the area. Based on the hourly temperature and humidity levels, it can be observed that the climate in the city of Oaxaca is hot during the summer and cold during the winter. The average annual temperature is 22 °C, with a range of 13.3 °C in September and 20 °C in February. Red dot lines in Figures 9 and 10 indicate the time for sunrise and sunset.

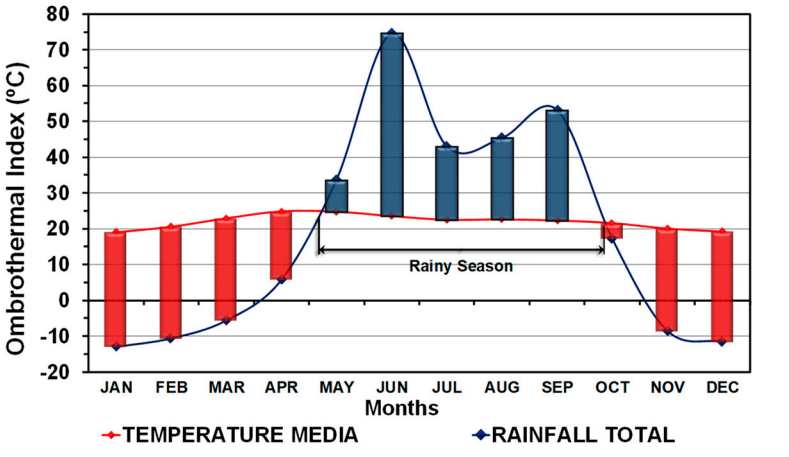

Figure 8. Rainy season in Oaxaca.

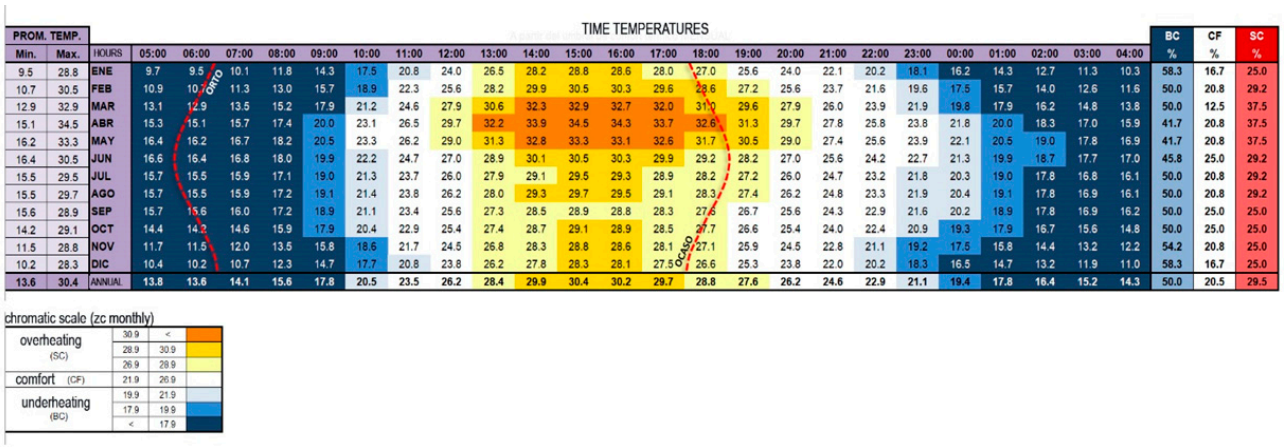

Figure 9. Hourly temperatures in Oaxaca.

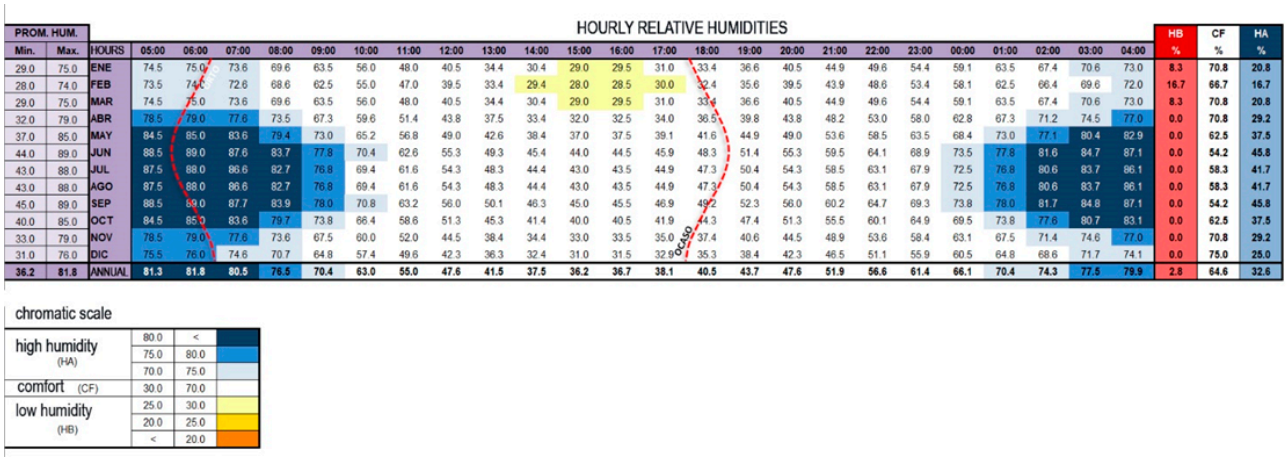

Figure 10. Hourly humidity in Oaxaca.

The data in Figure 11 are based on the psychrometric chart of Szokolay [28] from Software Climate Consultant 5.4, which is included in the EnergyPlusTM 2005, Design Builder Software Ltd. It uses an adaptive model applying the ASHRAE Standard. A climate file with an EPW extension generated in the Meteonorm software version 7.3 [29] was used for the input data. The Meteonorm software provides precise meteorological data for any location on Earth. It also has a program that calculates climatic parameters such as irradiation, temperature, humidity, wind, and precipitation. The software uses a dynamic methodology [30] that considers the user's thermal adaptation, which correlates with the type of clothing and the internal temperature. This information indicates that the clothing represents a measure of the user's adaptation.

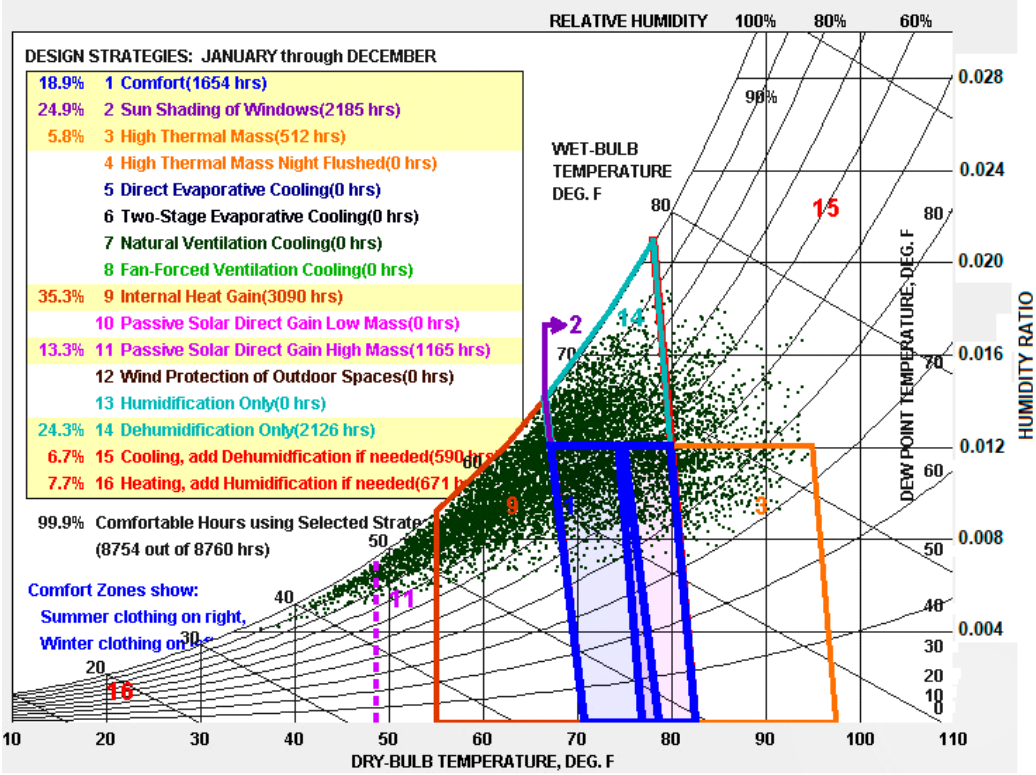

Figure 11. Psychrometric chart for Oaxaca.

The psychrometric chart analysis in Figure 11 shows that a 35.3% internal gain is required as a bioclimatic strategy for Oaxaca. This requirement is more pronounced in winter, particularly at night, with 24.9% window shading needed in March, April, and May 2023. Dehumidification is required by 24.3%, especially from June to September when the rainy season occurs.

The solar graph in Figure 12 for Oaxaca was developed using the Olgyay method [31], and it displays monthly data on azimuth angle and solar altitude. The yellow zone on the graph represents the overheating area, which is present throughout the year from 1:00 to 4:00 p.m. On the other hand, the blue zone represents the underheating area, present from 6 to 10 a.m., except for March and April, when it extends until 9 a.m.

Figure 13 shows the Evans comfort triangles [32], which indicate the thermal inertia for Oaxaca as a bioclimatic strategy for the entire year. The BAT bioclimatic analysis tool generated these triangles, which show temperature oscillations (variations throughout the day).

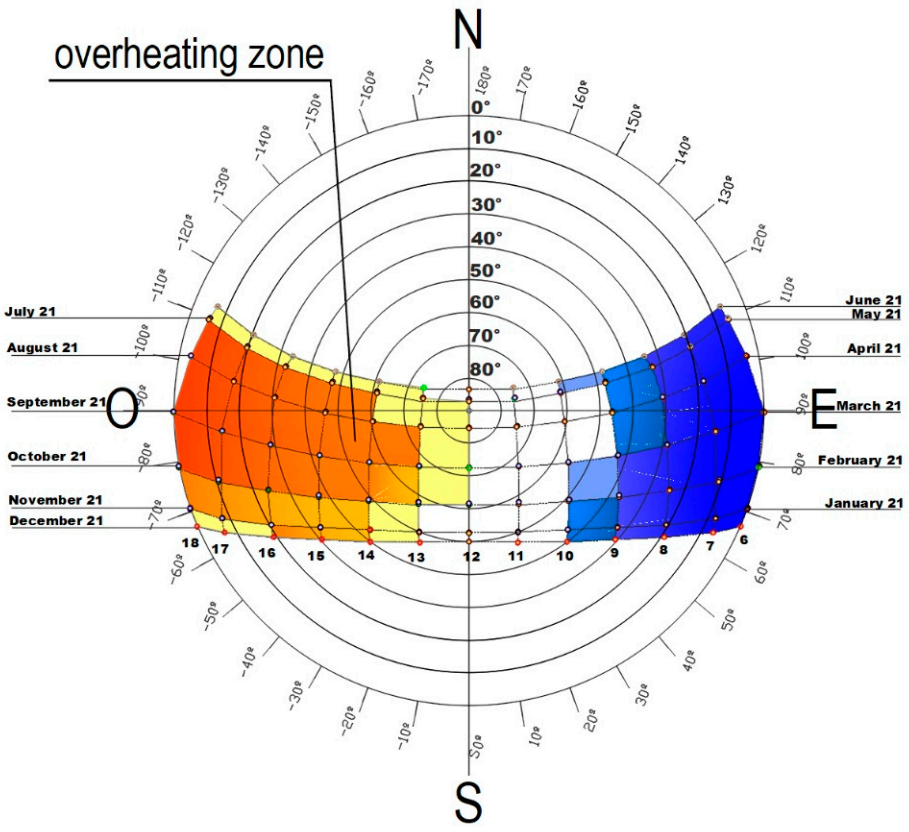

Figure 12. Olgyay's solar graph for Oaxaca.

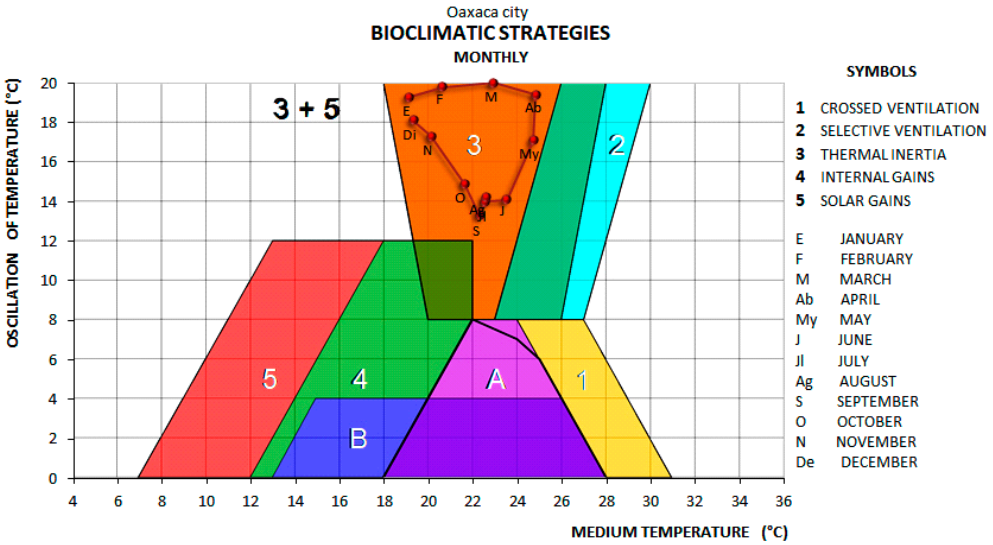

Figure 13. Evans' comfort triangle of Oaxaca.

3.2. Thermal Performance of Housing Prototypes

This section displays temperature measurements taken from inside the prototype housing. All the temperature records for the month studied (April 2023) were analyzed to determine the thermal comfort percentages and values above, below, or within the thermal comfort range.

According to Figure 14a, the MHTIT prototype system achieved 45% thermal comfort, 14.03% overheating, and 40.97% underheating. In Figure 14b, the MMLM construction system achieved 44.31% thermal comfort, 41.53% overheating, and 14.17% underheating. In Figure 14c, the MBSCLM construction system received 23% thermal comfort, 75.83%

overheating, and 1.1% underheating. Finally, in Figure 14d, the MMTLM constructive system had 48.06% thermal comfort, 43.61% overheating, and 8.33% underheating.

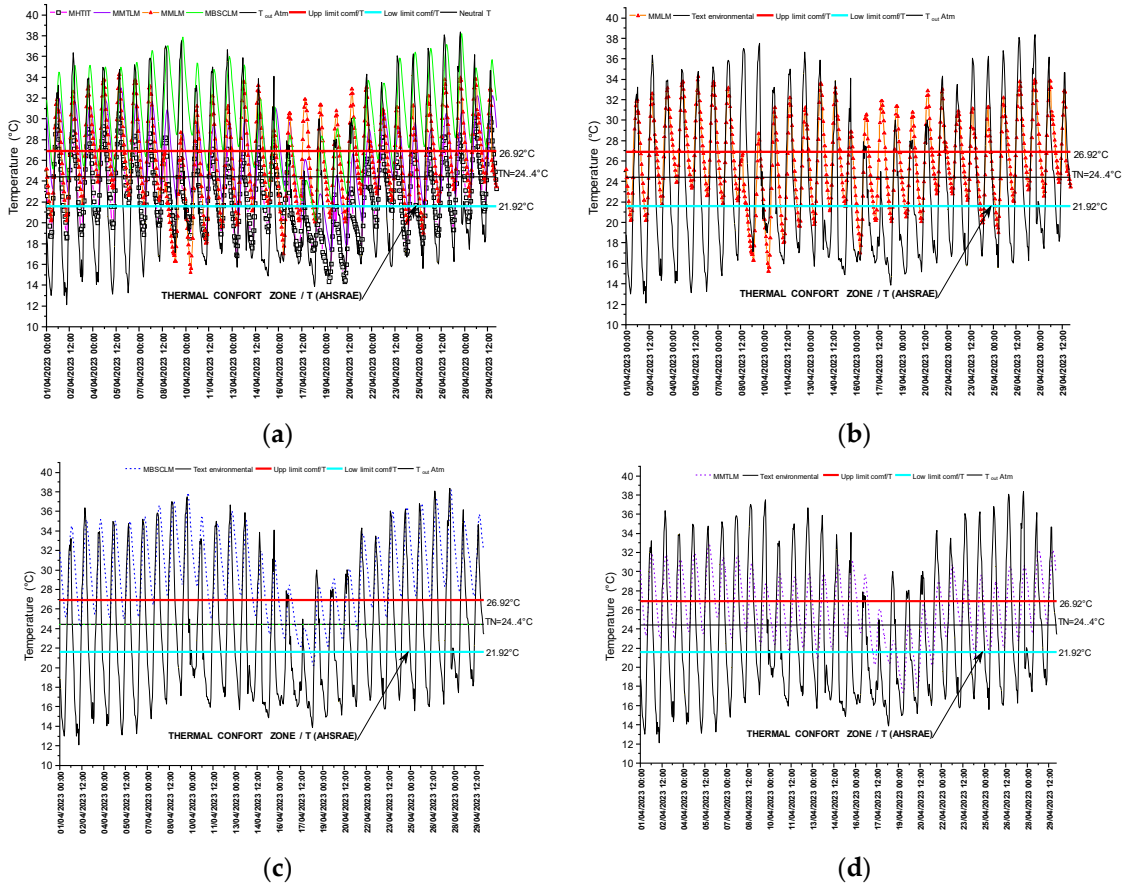

Figure 14. Interior temperatures in April 2023: (**a**) All four prototype systems: MHTIT, MMTLM, MMLM, and MBSCLM. (**b**) MMLM vs. T_{Ext}; (**c**) MBSCLM vs. T_{Ext}; (**d**) MMTLM vs. T_{Ext}.

Compared with other alternative construction systems in Figure 14a, the proposed MHTIT ecofriendly house prototype system achieved a similar thermal comfort percentage of 45%, except for the MBSCLM system, which had a low thermal comfort value. The MHTIT system had an advantage over the other house prototypes as it had the lowest overheating value. This indicates that the system's thermal inertia absorbed high temperatures from outside. However, the MHTIT system also had high temperatures below the thermal comfort range, as observed in Figure 14a.

Although the MHTIT system performed better than other systems in reducing the high outdoor temperatures, it did not fully maintain the interior temperatures within the thermal comfort range. To address this issue, a decision was made to modify the wall system of the MHTIT by adding a 2.5 cm thick layer of polystyrene insulation outside the wall with thermal mass. This modification helped to improve thermal comfort, and the modified prototype was named MHTITCA.

In this study, the MHTIT system was redesigned to obtain the MHTITCA system, and the temperature results are presented in Figure 15. The observations showed that the temperatures were mainly within the thermal comfort polygon, except for a few hours of low heating. The average daily temperature reduction was 5 °C compared to the MHTIT system that did not have insulation. The MHTITCA system reduced thermal oscillations outside, resulting in higher comfort during April compared to other systems. The insulation on the outside significantly reduced the fluctuations. As noted by Huelsz et al. [33], the position of the insulator affects the element's thermal performance, and the outside performs better than the inside. A building envelope with a high thermal storage

capacity and a correct layer array is also necessary. It is worth noting that a high thermal resistance value does not always guarantee good thermal performance.

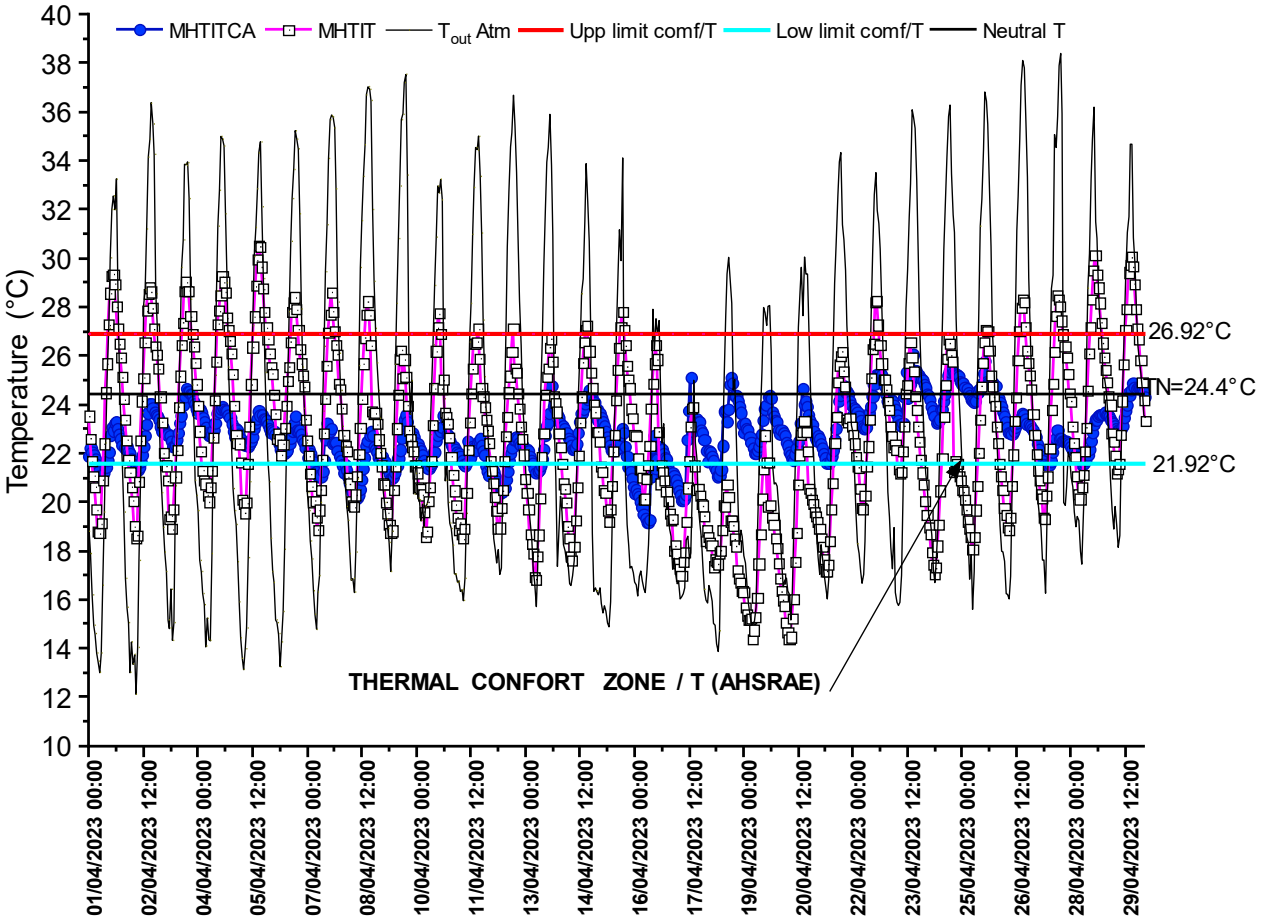

Figure 15. Comparative of the hybrid system with thermal insulation (MHTITCA) and without thermal insulation (MHTIT).

Based on a sample of 30 days of measurements during April 2023, with the input variables organized and classified with hourly and monthly temperature records that are only within the thermal comfort polygon, with a range of 21.6 °C as the lower limit of minimum temperature and 26.9 °C as the upper limit of maximum temperature, the data were analyzed using Minitab 18 software to obtain the results of the statistical tests of analysis of variance (ANOVA) and Tukey to get the average temperature of each home, as well as the mean standard error.

Table 1 shows the result of the statistical analysis of variance, where there is a 95% confidence that the MHTITCA prototype was the best option since it was significantly different from the other construction systems (this is shown with the letter B). It is also observed in the means (averages of the temperatures of the 30 days in the thermal comfort zone) with the lowest value (23.30). This is because more hours remained in the thermal comfort zone, as can be observed in column n, where it is shown that a more significant number of data were obtained per treatment. On the other hand, the MMTLM, MBSCLM, MMLM, and MHTIT systems were not significantly different, with MMTLM being the worst system. Finally, in the table showing the analysis of the variance, the *p*-value (test statistic) in the prototype model was 0.0001 and is much lower than 5.67 (F-value Fisher table), indicating that at least one of the treatments is different.

Table 1. Statistical analysis of variance and Tukey test.

AVERAGE					
Variable	N	R^2	R^2 Aj	CV	
Average	118	0.2	0.17	3.51	
Analysis of Variance Table (SC type III)					
F.V.	**SC**	**gl**	**CM**	**F**	***p*-valor**
Model	20.19	5	4.04	5.67	0.0001
Prototype	20.19	5	4.04	5.67	0.0001
Error	79.76	112	0.71		
Total	99.95	117			
Test: Tukey Alfa = 0.05 DMS = 0.80224, Error: 0.7121 gl: 112					
PROTOTYPE	**Median**	**n**	**E.E.**	**Comparison**	
MMTLM	24.57	18	0.2	A	
MBSCLM	24.27	24	0.17	A	
MMLM	24.14	21	0.18	A	
MHTIT	24.01	19	0.19	A	B
Outside Temperature	23.82	12	0.24	A	B
MHTITCA	23.3	24	0.17		B
Median values with a common letter are not significantly different ($p > 0.05$).					

Youcef Ettoumi et al. [9] recommend designing buildings with high thermal inertia to achieve comfortable room temperatures. However, thermal inertia is influenced by a complex interaction between the material, density, specific heat capacity, and thermal conductivity. The insulation material was crucial in reducing the external temperature in the current investigation.

The MHTITCA house system uses thermal inertia and low thermal conductivity to prevent overheating. It effectively dampens the external temperature by an average of 10 °C during the day while absorbing heat and increasing the outer wall temperature. The temperature drops considerably at night and remains comfortable, sometimes reaching the lower thermal threshold. Conversely, the outside temperature decreases at night without solar radiation.

A comparison of the thermal comfort of the eco-friendly house prototype MHTITCA and alternative prototypes in this work is summarized in Table 2. Results show that the MHTITCA system achieved 85% thermal comfort, with 0% overheating and 15% low heating. The MMTLM system obtained 48.06% thermal comfort, 43.61% overheating, and 8.33% low heating. The MBSCLM system had a thermal comfort of 23%, with 75.83% overheating and 1.1% low heating. Finally, the MMLM system achieved 44.31% thermal comfort, 41.53% overheating, and 14.17% underheating.

Table 2. Comparative graph of the housing prototypes under study.

Constructive System	Underheat (%)	Comfort (%)	Overheat (%)
MMLM	14	44	42
MBSCLM	1	23	76
MMTLM	8	48	44
MHTIT	14	45	41
MHTITCA	15	85	0

Overall, the MHTITCA system provided the highest thermal comfort compared to the other prototypes, with thermal comfort percentages for the MBSCLM, MMLM, and MMTLM systems being 76.94%, 47%, and 43%, respectively. The MHTITCA system also eliminated overheating, with only minimal underheating (15%).

Figure 16 illustrates an average day in April 2023, during which four different systems were compared regarding thermal oscillation. The MHTITCA system displayed the smallest thermal oscillation of 2.36 °C, whereas the MBSCLM, MMTLM, and MMLM systems showed thermal oscillations of 8.38 °C, 7.96 °C, and 13.87 °C, respectively. The average temperature remained constant at 22 °C across all systems. Figure 17 shows that the MHTITCA system with 0.20 m thick walls presented a thermal lag of 12 h.

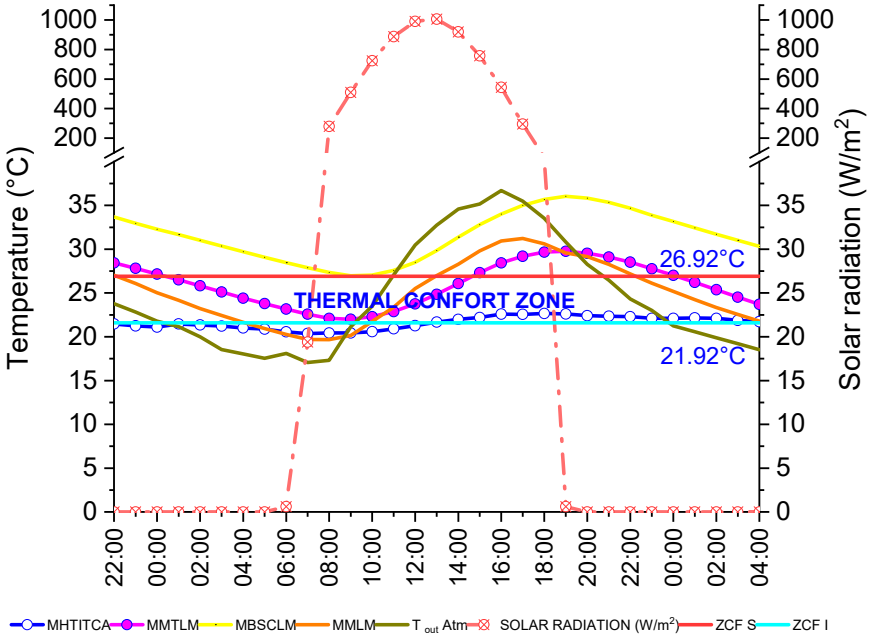

Figure 16. Hottest day of the systems under study.

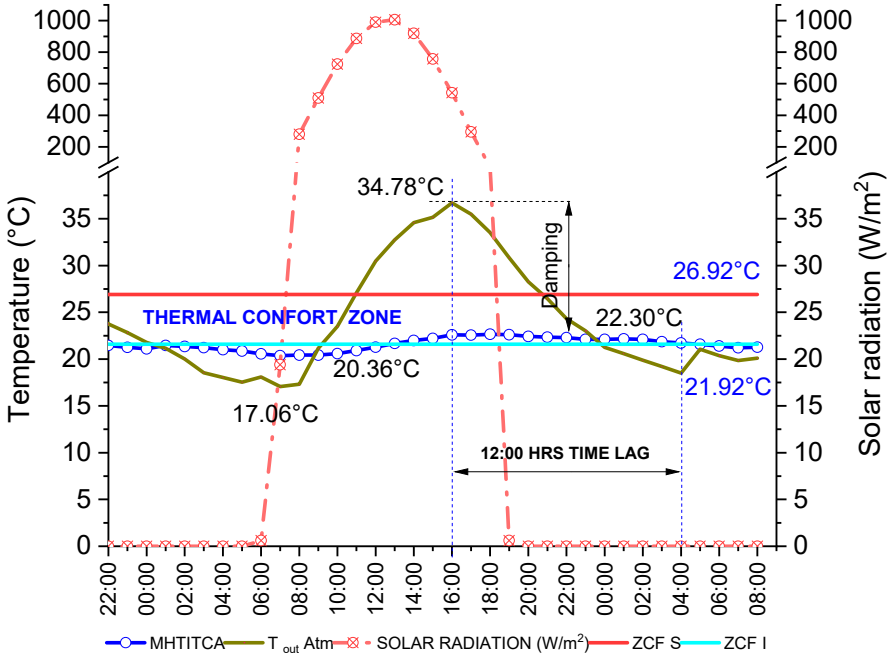

Figure 17. Thermal damping and time lag of the MHTITCA system.

Table 3 shows the MHTITCA house prototype system's decrement factor (0.109). This result is due to the system's properties, which integrate a soil–sawdust fiber matrix with a volumetric weight of 774.1 kg/cm^2 and a synergistic effect of thermal insulation on the outside of the wall, generating excellent thermal damping.

Table 3. Thermal amplitude and decrement factor.

System	Outside Surface Temperature Average Day in April			Inside Surface Temperature Average Day in April			Decrement Factor
	Temp Max (°C)	Temp Min (°C)	Δt Outside surface	Temp Max (°C)	Temp Min (°)	Δt Inside surface	
MHTITCA	34.78	17.06	17.72	22.3	20.36	1.94	0.109

Varini [34] suggested that the thermal gap should be 8 to 10 h so that the cold of the night is transmitted to the interior during the day and the heat is released to the exterior at night. The greater the mass, the greater the thermal inertia and, therefore, the better the thermal behavior [35]. The greater the thickness, density, specific heat, and resistivity of the enclosure materials, the greater the thermal retardation and damping. Acting together, these two factors cause both a reduction in heat fluxes and a delay when maximum surface temperatures are reached. The overall effect is stabilizing temperatures inside buildings to outside temperatures.

The results obtained in the MHTITCA system are very similar to the thermal lag indicated by Gallegos et al. [14], who analyzed a house with 0.4 m thick straw walls in Tecate, Baja California, Mexico. Their results showed a thermal lag of 9 to 12 h. This similarity in damping values may be due to the properties of the straw and wall thickness. On the other hand, the MHTITCA system exceeds the values obtained in experimental chambers by Belhadj et al. [36], where they investigated straw and cement walls with different thicknesses from 0.1 m to 0.25 m, obtaining thermal lag values from 4 to 8 h and a decrement factor from 0.15 to 0.85. On the other hand, Roux-Gutierrez and Velázquez Lozano [37] analyzed compressed earth blocks, obtaining a thermal lag of 4:15 h and a decrement factor of 2.28. Guillermo De Ignacio Vivens et al. [38] studied the thermal performance of walls. The results for the reinforced concrete panel with a thickness of 0.20 m obtained a thermal lag of 6.71 and a decrement factor of 0.17; for the concrete block wall with a thickness of 0.20 m, a thermal lag of 6.93 h was obtained. The perforated brick wall with a thickness of 0.24 m (greater than the MHTITCA system) showed a thermal lag of 7.72 h and a decrement factor of 0.13. In general, acceptable damping factors were obtained; however, since they do not have the thermal insulation layer considered in the MHTITCA system, they do not reach a higher level of damping.

Huelz et al. [33], in their simulations of time-dependent heat transfer, evaluated high-density concrete with an insulating layer of expanded polystyrene located in different positions, namely the outer, central, and inner parts. The results revealed that the function of the insulator is essential in the thermal performance of the element. The insulating layer in the inner part produces low damping and thermal time lag, while locating it in the outer part produces the best results, as in the MHTITCA system. Ulgen [39] highlights that the thermophysical properties and thickness of a building's opaque components can result in temporary delays of up to 12 h between external and internal temperatures. The insulating layer and thermal inertia function effectively in this regard. As a result, the interior temperature remained within the local thermal comfort polygon, as defined by Szokolay [27], throughout April, typically the hottest month of the year.

Table 4 shows the decrement factor results for each house prototype. The results were calculated based on the temperature difference between the maximum and minimum temperatures inside and outside the housing prototype. The prototypes were ranked in order of their decrement factor, with the best being MHTITCA (0.109), followed by MMTLM (0.425), MBSCLM (0.458), MHTIT (0.477), and finally MMLM (0.738).

Table 4. Decrement factor on an average day (April 2023's hottest week).

Prototype	ΔT_{In}	ΔT_{out}	Decrement Factor
MHTITCA	1.94	17.72	0.109
MHTIT	8.46		0.477
MBSCLM	8.12		0.458
MMTLM	7.54		0.425
MMLM	13.09		0.738

The thermal properties of the MHTITCA prototype were determined from the experimentally obtained equivalent thermal conductivity and analytical relationships, such as thermal conductance (TC), heat capacity (C), thermal admittance (Y), diffusivity (α), and effusivity (β), as shown in Table 5. From Table 5, the MHTITCA prototype was shown to exhibit the lowest values not only in decrement factor (0.109) and equivalent thermal conductivity (0.28 W/m K) but also in TC (1.08 W/m^2 K), heat capacity C (0.068 × 10^6 J/K), Y (1.08 W/m^2 K), β (271.81 $J{\cdot}m^{-2}{\cdot}K^{-1}{\cdot}s^{-0.5}$), and thermal diffusivity α (1.098 × 10^{-6} $m^2{\cdot}s^{-1}$), as well as the highest values of thermal time lag (12:00 h) from the real-scale prototypes tested.

Table 5. Main thermal properties for MHTITCA.

Part	λ (W/m K)	TC (W/m^2 K)	C (J/K) ×10^6	Y ($W/m^2{\cdot}K$)	α ($m^2{\cdot}s^{-1}$) ×10^{-6}	β ($J{\cdot}m^{-2}{\cdot}K^{-1}{\cdot}s^{-0.5}$)	ρ (kg/m^3)	Ms (kg/m^3)	L (m)
MHTITCA	0.28	1.08	0.068	1.08	1.098	271.81	1285.38	340.625	0.265

Values of λ (equivalent thermal conductivity), TC (thermal conductance), C (heat capacity), Y (thermal admittance), α (diffusivity), β (effusivity), ρ (density), Ms (mass density), L (thickness).

Heat capacity represents the ability of a material to store heat while undergoing a given temperature change. Thermal effusivity measures its ability to exchange heat with its surroundings, and in MHTITCA, it was very low and warm to the touch. MHTITCA registered a low diffusivity, which means it is a material that could prevent fast heat exchange with the environment. Thus, if thermal inertia is understood in terms of thermal effusivity, a material with high thermal inertia (MHTITCA) would not change its temperature as drastically as one with low thermal inertia.

4. Discussion

Relevance and Significance of the Current Study

Measurements in real-scale house prototypes are very important and helpful when you want to know the thermal comfort of a building relative to the local comfort polygon. The material's or component's thermal properties alone cannot tell us anything in that direction. In the literature, there are very few experimental studies on thermal lag and decrement factor in real-scale house prototypes, which is why the comparison carried out was against the constructive components reported in the past.

Table 6 presents the results of past studies on thermal inertia (decrement factor and thermal lag) in construction components compared against this work on the eco-friendly MHTITCA house prototype that uses a reinforced mortar channel filled with soil–sawdust fiber–cement plus insulation in the envelope of walls and ceilings of the prototype built at real scale. These results were 12 h of thermal lag and a 0.109 decrement factor. These outstanding values provided 85% thermal comfort inside the house prototype. In this sense, a construction system with high thermal inertia in the walls and ceilings, as used in the MHTITCA house prototype based on a reinforced mortar channel filled with soil–sawdust fiber–cement + 2.5 cm polystyrene, provided the greatest thermal comfort against the

alternative house prototypes evaluated in the present work, as well as past work by other authors, as indicated in Table 6.

Table 6. Thermal lag and decrement factor. A comparison between previous studies and the current study.

Wall Type	Thermal Lag (H)	Decrement Factor	References
Component of reinforced mortar channel filled with cement–soil (18 cm thick)	7.5	0.16	[40]
MHTITCA real-scale house prototype prefabricated channel of reinforced mortar filled with soil–sawdust fiber–cement combined with insulation (20.5 cm thick)	12	0.109	This work
Simple compressed earth block with plaster (16.5 cm thick)	1.5	1.807	[41]
Double compressed earth block (BTC) with plaster (30.5 cm thick)	4.25	2.162	[41]
Baked clay brick (14 cm thick)	0.5	1.561	[41]
Concrete block (14 cm thick)	0.5	1.886	[41]
Extensive green roof (29 cm thick)	8.5	0.098	[42]
Brick wall with plaster on both sides plus polyurethane insulation on the outside (33 cm thick)	12.275	0.009	[43]
Cellular concrete (15 cm thick)	4.837	0.104	[43]
Dense concrete (15 cm thick)	2.512	0.488	[43]
Concrete with plaster on both sides (24 cm) with expanded polystyrene insulation (5 cm), total thickness of 29 cm	7.04	0.0157	[44]
Straw and cement walls with thicknesses of 10 to 25 cm	4 to 8	0.15 a 0.85	[36]
Straw bale walls 40 cm thick	9	Not reported	[14]

Figure 18 compares the variation of the decrement factor according to the thickness of the material wall studied by various authors. The reduction in the decrement factor defines the materials' thermal storage capacity. In the case of the MHTITCA house prototype, the thermal inertia of the clay and the sawdust fiber, whose thermal conductivity is low, were combined. The decrement factor increased for materials that do not have thermal insulation (dense concrete, baked clay brick, compressed earth block with plaster, concrete block, and compressed earth block with plaster), for example, in studies [45,46].

Figure 19 shows an increase in thermal damping with increasing component thickness. This is more evident with thicker materials, such as hybrid MHTITCA components, concrete with plaster on both sides + 0.5 m insulation on the outside, brick walls with plaster on both sides plus polyurethane insulation on the outside, cellular concrete, extensive green roofs, hybrid construction components, concrete with plaster on both sides + 0.5 m insulation on the outside, and compressed earth blocks with plaster. For materials with smaller thicknesses and without a layer of thermal insulation (dense concrete, compressed earth blocks with plaster, concrete blocks, and baked clay bricks), the thermal lag was low, for example, in [45,46].

Insulating the exterior of a wall in a house prototype creates a continuous layer that covers the entire surface. This insulation layer is more effective when placed outside the wall in preventing heat transfer than when insulation is placed inside the wall because there are no breaks or gaps in the layer. The exterior insulation layer is also protected from the elements, which can damage or degrade insulation over time. When insulation is placed inside a wall, it is often compressed between the framing members and the wall surface. Compression tends to reduce the insulation's thermal resistance and create gaps and voids in the insulation layer, transferring heat through the wall. This can make the insulation less effective in slowing down heat transfer. Putting insulation on the outside of a wall

creates a more efficient thermal barrier, such as air and moisture, between the interior of the house and the outside environment. This barrier helps to maintain a consistent temperature inside the house by preventing heat from entering during summer and escaping during winter. This reduces the amount of energy required to heat or cool the space. As a result, the prototype house's overall energy consumption can be reduced, while the comfort of the occupants can be improved.

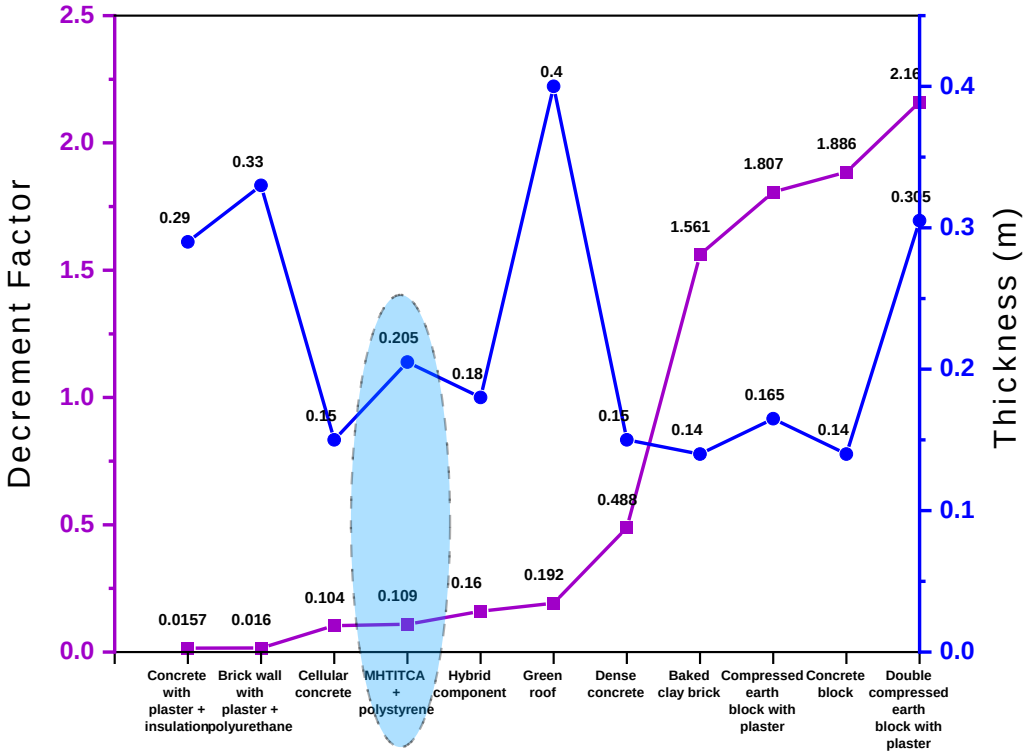

Figure 18. Decrement factor and wall thickness of the present study vs. past studies.

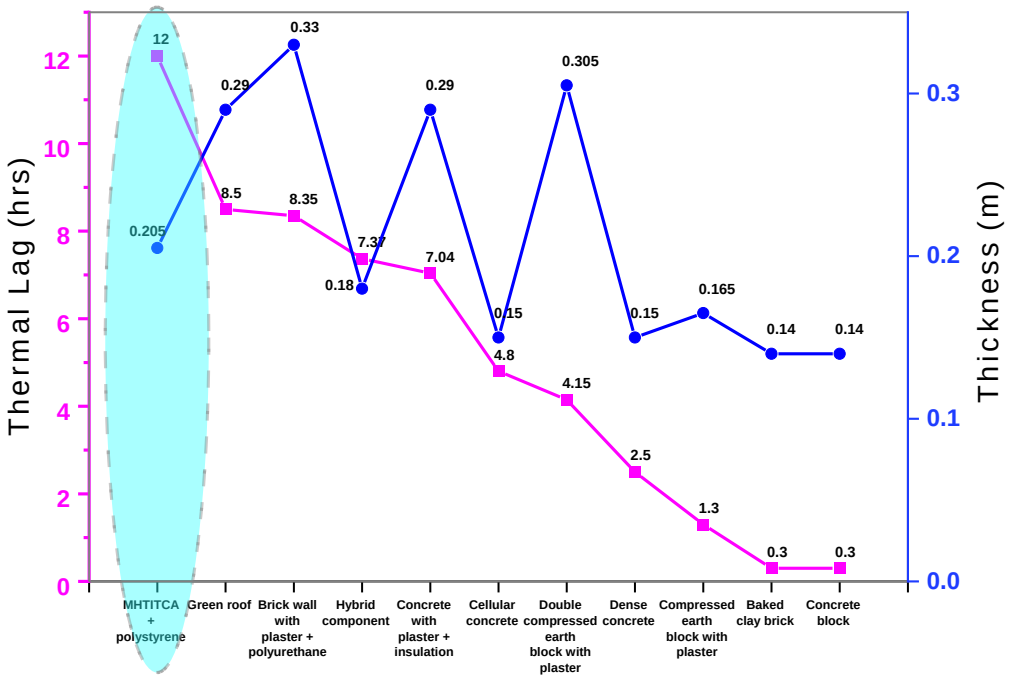

Figure 19. Thermal lag and wall thickness vs. past studies.

Since heat transfer occurs through a conduction process in solid materials such as insulation, at a molecular level, atoms and molecules vibrate to transfer heat. Placing insulation on the exterior of a wall slows down the movement of these atoms and molecules, which in turn slows down the transfer of heat. The insulation material comprises millions of tiny pockets that trap air, an inferior conductor of heat. These pockets create a barrier that helps to slow the transfer of heat energy through the material. When insulation voids are compressed or trapped air pockets are eliminated, the insulation's effectiveness is reduced. Additionally, when heat is conducted through structural elements such as framing members, it creates a thermal bridge that allows heat to transfer through the wall, reducing the overall effectiveness of the insulation. Placing insulation on the exterior of the building helps to reduce thermal bridging, as the thermal bridge is eliminated.

5. Conclusions

A real-scale eco-friendly prototype house was built at CIIDIR facilities in Oaxaca City, Oaxaca, Mexico. This research showcases the findings of a full-scale experimental house prototype, MHTITCA. It features a distinctive design that combines prefabricated modular reinforced channels filled with soil, sawdust fiber, and cement, incorporating an insulating layer in the external wall of the house prototype system for both walls and roofs. It can be concluded that the MHTITCA prototype also highlights a thermal time lag of 12 h, an ability to achieve 85% thermal comfort, a minimal decrement factor of 0.109, and zero overheating in areas with high thermal fluctuations. These metrics are significant as they showcase the prototype's effectiveness in managing thermal fluctuations, which is crucial for regions with high-oscillation temperate climates. Comparatively, the other prototypes examined provided inferior thermal comfort. This result is important because it means that the MHTITCA filling mixture of the prefabricated channels plus insulation limits the heat flow at peak times when temperatures reach their highest values.

Based on the results, it is evident that housing in areas with high thermal oscillations requires improvements in terms of thermal inertia and insulation. A real-scale prototype provides practical insights into the system's performance, offering more robust data than smaller-scale or theoretical models. The proposed MHTITCA house prototype can provide an ecological alternative for energy saving and thermal comfort, especially in temperate climates with high thermal oscillations in urban and rural areas. Further research will focus on enhancing the prototype's thermal performance by adding phase change materials and utilizing different combinations in its layers, focusing on the prototype's long-term thermal performance all year in cold or hot climates in other climatic regions of Mexico.

Author Contributions: Conceptualization, R.A.-R. and F.C.-C.; Methodology, R.A.-R.; Validation, F.C.-C.; Formal analysis, R.A.-R. and M.C.-C.; Investigation, J.M.-R., R.A.-R., M.O.-G., V.J.M.-D. and J.L.C.-M.; Resources, R.A.-R. and M.C.-C.; Writing—original draft, R.A.-R. and F.C.-C.; Writing—review & editing, F.C.-C., M.C.-C., E.A.J.-A., L.E.S.-D.l.R. and L.H.R.-T.; Supervision, M.C.-C. and F.C.-C. All authors have read and agreed to the published version of the manuscript.

Funding: This research was funded by Instituto Politecnico Nacional IPN Project SIP-20242121.

Institutional Review Board Statement: Not applicable.

Informed Consent Statement: Not applicable.

Data Availability Statement: The original contributions presented in the study are included in the article; further inquiries can be directed to the corresponding author.

Acknowledgments: The authors wish to express their sincere thanks to the National Council of Humanities, Sciences, and Technologies (Conahcyt), Secretary of Public Education (SEP), Instituto Politecnico Nacional (IPN), and TecNM/Instituto Tecnologico de Oaxaca for the financial support they received to carry out the present work.

Conflicts of Interest: The authors declare no conflicts of interest.

References

1. Tsitoura, M.; Michailidou, M.; Tsoutsos, T. A Bioclimatic Outdoor Design Tool in Urban Open Space Design. *Energy Build.* **2017**, *153*, 368–381. [CrossRef]
2. Frank, A.A.; Kuchen, E. Validación de La Herramienta Metodológica de Alonso-Frank & Kuchen Para Determinar El Indicador de Nivel de Eficiencia Energética Del Usuario de Un Edificio Residencial En Altura, En San Juan—Argentina. *Rev. Hábitat Sustentable* **2017**, *7*, 6–13.
3. Manzano-Agugliaro, F.; Montoya, F.G.; Sabio-Ortega, A.; García-Cruz, A. Review of Bioclimatic Architecture Strategies for Achieving Thermal Comfort. *Renew. Sustain. Energy Rev.* **2015**, *49*, 736–755. [CrossRef]
4. Wegertseder, P.; Schmidt, D.; Hatt, T.; Saelzer, G.; Hempel, R. Barreras y Oportunidades Observadas En La Incorporación de Estándares de Alta Eficiencia Energética En La Vivienda Social Chilena. *Arquit. Urban.* **2014**, *35*, 37–49.
5. *ISO7730:2005*; Ergonomics of the Thermal Environment-Analytical Determination and Interpretation of Thermal Comfort Using Calculation of the PMV and PPD Indices and Local Thermal Comfort Criteria. International Organization for Standardization: Geneva, Switzerland, 2005.
6. *ANSI/ASHRAE 55:2004*; Thermal Environmental Conditions for Human Occupancy. ASHRAE: Peachtree Corners, GA, USA, 2004.
7. Maldonado, E.; Yannas, S.; Gonçalves, H. Studies of the Thermal Performance of Buildings in Summer in Southern Europe. *Int. J. Sol. Energy* **1997**, *19*, 161–178. [CrossRef]
8. Czajkowski, J.D.; Gómez, A.F.; Gracia Bianciotto, M. Comportamiento Térmico de Viviendas Sociales Mediante Incorporación de Mejoras de Diseño En La Envolvente. *Av. Energírenov. Medio Ambiente* **2008**, *12*, 33–40.
9. Youcef Ettoumi, F.; Messen, N.; Adane, A.E.H.; Sauvageot, H. Temperature Variations in a Housing of the Semi-Arid Region of Djelfa (Algeria). *Build. Environ.* **2003**, *38*, 511–519. [CrossRef]
10. Karlsson, J.; Wadsö, L.; Öberg, M. A Conceptual Model That Simulates the Influence of Thermal Inertia in Building Structures. *Energy Build.* **2013**, *60*, 146–151. [CrossRef]
11. Alavéz-Ramírez, R.; Chiñas-Castillo, F.; Morales-Domínguez, V.J.; Ortiz-Guzmán, M.; Caballero-Montes, J.L.; Caballero-Caballero, M. Thermal Lag and Decrement Factor of Constructive Component Reinforced Mortar Channels Filled with Soil–Cement–Sawdust. *Indoor Built Environ.* **2018**, *27*, 466–485. [CrossRef]
12. Filippín, C.; Flores Larsen, S. Comportamiento Termico de Verano de Viviendas Unifamiliares Compactas En Condiciones Reales de Uso En Clima Templado En Argentina. *Av. Energías Renov. Medio Ambient.* **2010**, *14*, 1–8.
13. Flores, L.S.; Flores Larsen, S.; Filippín, C. Comportamiento Térmico de Invierno y Verano de Viviendas de Interes Social En La Provincia de Salta. *Av. Energías Renov. Medio Ambient.* **2007**, *11*, 167–173.
14. Gallegos-Ortega, R.; Magaña-Guzmán, T.; Reyes-López, J.A.; Romero-Hernández, M.S. Thermal Behavior of a Straw Bale Building from Data Obtained in Situ. A Case in Northwestern México. *Build. Environ.* **2017**, *124*, 336–341. [CrossRef]
15. Medjelakh, D.; Abdou, S. Impact de l'inertie Thermique Sur Le Confort Hygrothermique et La Consommation Énergétique Du Bâtiment. *Rev. Des Energies Renouvelables* **2008**, *11*, 329–341. [CrossRef]
16. Norén, A.; Akander, J.; Isfält, E.; Söderström, O. The Effect of Thermal Inertia on Energy Requirement in a Swedish Building—Results Obtained with Three Calculation Models. *Int. J. Low Energy Sustain. Build.* **1999**, *1*, 1–16.
17. Shaviv, E.; Yezioro, A.; Capeluto, I.G. Thermal Mass and Night Ventilation as Passive Cooling Design Strategy. *Renew. Energy* **2001**, *24*, 445–452. [CrossRef]
18. Givoni, B. Effectiveness of Mass and Night Ventilation in Lowering the Indoor Daytime Temperatures. Part I: 1993 Experimental Periods. *Energy Build.* **1998**, *28*, 25–32. [CrossRef]
19. Ogoli, D.M. Predicting Indoor Temperatures in Closed Buildings with High Thermal Mass. *Energy Build.* **2003**, *35*, 851–862. [CrossRef]
20. Aste, N.; Angelotti, A.; Buzzetti, M. The Influence of the External Walls Thermal Inertia on the Energy Performance of Well Insulated Buildings. *Energy Build.* **2009**, *41*, 1181–1187. [CrossRef]
21. Filippín, C.; Flores Larsen, S.; Flores, L. Comportamiento Energetico de Verano de Una Vivienda Masica y Una Liviana En La Region Central de Argentina. *Av. Energías Renov. Medio Ambient.* **2007**, *11*, 17–23.
22. Fuentes Freixanet, V. *Mapas Bioclimáticos de La República Mexicana*, 1st ed.; Universidad Autónoma Metropolitana: México City, Mexico, 2014.
23. SMN Normales Climatológicas, Comisión Nacional Del Agua. Available online: https://smn.conagua.gob.mx/tools/RESOURCES/Normales_Climatologicas/Normales9120/oax/nor9120_20079.txt (accessed on 26 October 2024).
24. Bahar, R.; Benazzoug, M.; Kenai, S. Performance of Compacted Cement-Stabilised Soil. *Cem. Concr. Compos.* **2004**, *26*, 811–820. [CrossRef]
25. Roseto, O. Bloques Con Mezclas Hipercomprimidas de Suelo-Cemento. *Rev. Cem.* **1996**, *6*, 11–13.
26. *NMX-C-037-ONNCCE*; Building Industry Concrete, Blocks, Bricks or Partition Masonry Wits Units Determination of Absorbent Water and Determination of Initial Absorbent. Industria de la construcciOn-Bloques: San Francisco, CA, USA, 2005.
27. Auliciems, A.; Szokolay, S.V. *Thermal Comfort*, 2nd ed.; PLEA NOTE 3 Passive and Low Energy Architecture International: Chapel Hill, Australia, 1985; ISBN 0-86776-729-4.
28. Szokolay, S.V. *Introduction to Architectural Science: The Basis of Sustainable Design*, 2nd ed.; Elsevier Ltd.: Oxford, UK, 2008; ISBN 0-7506-58495.

29. Meteotest Meteonorm. *Global Meteorological Database for Engineers, Planners and Education*; Edition 2020 Software and Data Cd-Rom. Meteonorm: Bern, Switzerland, 2020.
30. De Dear, R.; Brager, G.S. The Adaptive Model of Thermal Comfort and Energy Conservation in the Built Environment. *Int. J. Biometeorol.* **2001**, *45*, 100–108. [CrossRef] [PubMed]
31. Olgyay, V. *Design with Climate: Bioclimatic Approach to Architectural Regionalism: New and Expanded Edition*, 2016th ed.; Princeton University Press: Princeton, NJ, USA, 2015; ISBN 9781400873685.
32. Evans, J.M.; de Schiller, S. *Diseño Bioambiental y Arquitectura Solar.*, 3rd ed.; FADU, UBA, Buenos Aires, Argentina: Buenos Aires, Argentina, 1994; ISBN 950-29-0037-5.
33. Huelsz, G.; Barrios, G.; Rechtman, R.; Rojas, J. Importancia Del Análisis de Transferencia de Calor Dependiente Del Tiempo En La Evaluación Del Desempeño Térmico de La Envolvente de Una Edificación. *Estud. Arquit. Bioclimática* **2011**, *9*, 9–19.
34. Varini, C. *Ecoenvolventes: Entre Continuidad e Innovacion*, 1st ed.; Universidad Piloto de Colombia: Bogota, Colombia, 2016; ISBN 9789588957364.
35. De Garrido, L. *Manual de Arquitectura Ecológica Avanzada*, 1st ed.; Ediciones de la U: Bogota, Colombia, 2017; ISBN 9789587627053.
36. Belhadj, B.; Bederina, M.; Makhloufi, Z.; Goullieux, A.; Quéneudec, M. Study of the Thermal Performances of an Exterior Wall of Barley Straw Sand Concrete in an Arid Environment. *Energy Build.* **2015**, *87*, 166–175. [CrossRef]
37. Roux-Gutiérrez, R.S.; Velázquez Lozano, J. Bloques de Tierra Comprimida, Su Retardo Térmico e Impacto Ambiental. *Rev. Legado Arquit. Diseño* **2016**, *19*, 81–90.
38. De Ignacio Vivens, G.; Soutullo Castro, S.; López-Zaldivar, O.; Lozano-Diez, R.V.; Verdú Vázquez, A. Sobre Inercia Térmica y Aislamiento de Viviendas En Clima Cálido-Húmedo = On Thermal Inertia and Insulation of Buildings in Warm-Humid Climate. *An. Edif.* **2018**, *4*, 14–26. [CrossRef]
39. Ulgen, K. Experimental and Theoretical Investigation of Effects of Wall's Thermophysical Properties on Time Lag and Decrement Factor. *Energy Build.* **2002**, *34*, 273–278. [CrossRef]
40. Alavéz-Ramírez, R.; Chiñas-Castillo, F.; Caballero-Caballero, M.; Juventino Morales-Domínguez, V.; Ortiz-Guzmán, M.; Eugenia Silva-Rivera, M.; Candido Jimenez-Piñon, R.; Ramos-Alonso, A. Sugar Cane Products as a Sustainable Construction Material—Case Study: Thermophysical Properties of a Corncob and Cane Bagasse Ash Panel. In *Sugarcane—Its Products and Sustainability*; Kumar Ghimire, B., Ed.; IntechOpen: London, UK, 2023; pp. 1–22, ISBN 978-1-80356-369-5.
41. Roux Gutierrez, R.S.; Gallegos Sanchez, D.P. Construccion Sustentable, Analisis de Retraso Termico a Bloques de Tierra Comprimidos. *Context. Rev. Fac. Arquit. Univ. Autónoma Nuevo León* **2015**, *9*, 59–71.
42. Bevilacqua, P.; Mazzeo, D.; Arcuri, N. Thermal Inertia Assessment of an Experimental Extensive Green Roof in Summer Conditions. *Build. Environ.* **2018**, *131*, 264–276. [CrossRef]
43. Balaji, N.C.; Mani, M.; Venkatarama Reddy, B.V. Thermal Performance of the Building Walls. *Build. Simul. Appl.* **2013**, *346*, 151–159.
44. Ozel, M.; Ozel, C. Comparison of Thermal Performance of Different Wall Structures. In Proceedings of the HEFAT2012 9th International Conference on Heat Transfer, Fluid Mechanics and Thermodynamics, Hefat, Malta, 16–18 July 2012; pp. 674–679.
45. Humaish, H.; Marmoret, L.; Beji, H. Effect of Thermal Inertia (Time Lag and Decrement Factor) on the Insulation Thermal Capacity. In Proceedings of the 2018 International Conference on Advance of Sustainable Engineering and its Application (ICASEA), Wasit-Kut, Iraq, 14–15 March 2018; pp. 137–141. [CrossRef]
46. Asan, H.; Sancaktar, Y.S. Effects of Wall's Thermophysical Properties on Time Lag and Decrement Factor. *Energy Build.* **1998**, *28*, 159–166. [CrossRef]